Chaos and multifractality in a time-delay car-following traffic model

Leonid A. Safonov[1,2], Elad Tomer[1], Vadim V. Strygin[2], Yosef Ashkenazy[3], and Shlomo Havlin[1]

[1] Minerva Center and Department of Physics,
Bar–Ilan University, 52900 Ramat–Gan, Israel
[2] Department of Applied Mathematics and Mechanics,
Voronezh State University, 394693 Voronezh, Russia
[3] Center for Global Change Science,
Massachusetts Institute of Technology, Cambridge, Massachusetts 02139, USA

Abstract. The presence of chaos in traffic is studied using a car-following model based on a system of delay-differential equations. We find that above a certain time delay and for intermediate density values the system passes to chaos following the Ruelle-Takens-Newhouse scenario (fixed point – limit cycles – two-tori – three-tori – chaos). Exponential decay of the power spectrum and positive Lyapunov exponents support the existence of chaos. We find that the chaotic attractors are multifractal.

1 Introduction

Traffic flow often exhibits irregular and complex behavior. It was observed experimentally (e.g. [1]), that although for low and high cars density the motion is relatively simple, for intermediate density values (in the so called "synchronized flow phase" [1]) the motion is characterized by abrupt changes in cars velocities and flow flux. Here we study a model based on a system of delay-differential equations, which for sufficiently large delay and intermediate density values demonstrates complex behavior, attributed to the presence of chaos.

The presence of chaotic phenomena in traffic models has been reported in recent studies. Addison and Low [2] observed chaos in a single-lane car-following model in which a leading car has oscillating velocity. Nagatani [3] reported the presence of a chaotic jam phase in a lattice hydrodynamic model derived from the optimal velocity model [4].

Unlike the above studies, our model is based on a system of autonomous delay-differential equations, and the transition to chaos is possible only in the presence of delay. We show that the system can pass to chaos via many similar routes, and that many different non-chaotic and chaotic attractors may coexist for the same parameter values. We also observe multifractality of the chaotic attractor, which is novel in traffic studies.

We generalize the model proposed and studied in [5–7] by introducing time delay τ in the driver's reaction. The preliminary results of the present study can be found in [8].

The model is based on the assumption that N cars move in a single lane and the nth car motion is described by the delay-differential equation

$$\frac{d^2x_n(t)}{dt^2} = A\left(1 - \frac{\Delta x_n^0(t-\tau)}{\Delta x_n(t-\tau)}\right) - \frac{Z^2(-\Delta v_n(t-\tau))}{2(\Delta x_n(t-\tau) - D)} - kZ(v_n(t-\tau) - v_{per}), \tag{1}$$

where $n = 1, \ldots, N$, x_n is the car's coordinate, v_n – its velocity, A and k – sensitivity parameters, D – minimal distance between consecutive cars, v_{per} – permitted velocity, T – safety time gap, $\Delta x_n^0 = v_n T + D$ the safety distance, $\Delta x_n = x_{n+1} - x_n$ and $\Delta v_n = v_{n+1} - v_n$. The function Z is defined as $Z(x) = x$ for $x > 0$ and $Z(x) = 0$ for $x \le 0$. In our computations we use the parameters values $v_{per} = 25(m/s)$, $T = 2(s)$, $D = 5(m)$, $A = 3(m/s^2)$, $k = 2(s^{-1})$ and $N = 100$. The boundary conditions are periodic, i. e. $x_{N+1} = x_1 + L$, $v_{N+1} = v_1$, where L is the road length.

In this study we find that for sufficiently large delay the system behaves in a complex manner. We show numerically, that the above mentioned limit cycles may bifurcate into two-dimensional tori. With further change of density the tori bifurcate into three-dimensional tori, which are subsequently destroyed forming chaotic attractors. This scenario is known as Ruelle-Takens-Newhouse route to chaos [9].

2 Transition to Chaos

To study the transition to chaos we first consider the following solution of system (1)

$$v_n^0 = v^0 = \begin{cases} \frac{A(1-D\rho)+kv_{per}}{A\rho T+k}, & \rho \le \frac{1}{D+Tv_{per}}, \\ \frac{1-D\rho}{\rho T}, & \rho > \frac{1}{D+Tv_{per}}, \end{cases} \qquad x_n^0 = \frac{n-1}{\rho} + v^0 t, \tag{2}$$

where $\rho = N/L$ is the cars density. This solution corresponds to the homogeneous flow, in which all cars have the same velocity and headways are equal. We introduce a new variable $\xi_n = \Delta x_n - 1/\rho$ in Eq. (1). By this change of variables the homogeneous flow solution (2) is mapped to zero. Its stability can be analyzed using the linearization of Eqs. (1)

$$\ddot{\xi}_n^0(t) = -p\dot{\xi}_n^0(t-\tau) + q\big(\xi_{n+1}^0(t-\tau) - \xi_n^0(t-\tau)\big), \tag{3}$$

where $p = AT\rho + k$, $q = \frac{AT+kTv_{per}+kD}{AT\rho+k} \cdot A\rho^2$ if $\rho \le \frac{1}{D+Tv_{per}}$ and $p = AT\rho$, $q = A\rho$ otherwise.

Following [4,5], we look for a solution of equations (3) in the form

$$\xi_n^0 = \exp(i\alpha_\kappa n + \lambda t), \tag{4}$$

where $\alpha_\kappa = \frac{2\pi}{N}\kappa$ ($\kappa = 0, \ldots, N-1$) and λ is a complex number. Substituting (4) into (3) we obtain a set of algebraic equations for λ

$$\lambda^2 + [p\lambda - q(e^{i\alpha_\kappa} - 1)]e^{-\lambda\tau} = 0. \tag{5}$$

The solutions of Eqs. (5) are the eigenvalues of system (3). One of these solutions (for $\kappa = 0$) is zero. The others have negative real part for sufficiently high and sufficiently low values of ρ, which indicates the stability of the homogeneous flow solution. As ρ decreases (increases), pairs of complex eigenvalues may cross the imaginary axis, causing the formation of small limit cycles (Hopf bifurcations).

We study the formation of limit cycles with the density decreasing from high to intermediate values. Let for some $\rho = \rho_0$ Eqs. (5) with some κ have a pair of purely imaginary solutions (a Hopf bifurcation point). For $\rho = \rho_0 - \varepsilon$ we find the newly-born limit cycle in the form $\xi_n(t) \sim \varepsilon\xi_n^0(t)$, using an approximate technique similar to that used in [7] for the non-delay case. Obviously, the flow state corresponding to this limit cycle is a wave with the wavelength equal to L/κ (in length units) or N/κ (in number of cars).

After the small limit cycle for density close to the Hopf bifurcation value is found analytically, its global continuation is performed numerically in the following manner. For $\rho \approx \rho_0 - \varepsilon$ we take the analytically found approximate periodic solution as an initial condition and solve Eqs. (1) numerically. After the solution has reached an attracting set, we decrease ρ with a small step and solve the equations numerically again, taking the results from the previous step as initial conditions. This procedure is iterated further. In this way we keep the track of the particular limit cycle.

For the non-delay case [7] we have not found any other attracting sets than limit cycles and fixed points. With a small delay the system's behavior

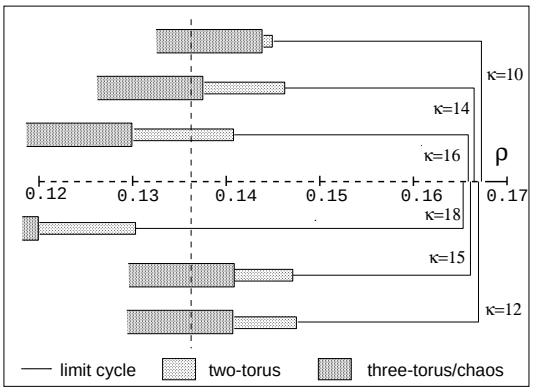

Fig. 1. A schematic bifurcation diagram, showing transition to chaos from six different limit cycles. The figure shows that limit cycles, two-tori and chaotic attractors can coexist for the same parameter values (see the vertical dashed line).

does not change qualitatively. For higher values of τ (above approximately $0.5(s)$) the cycles may undergo bifurcations leading to the transition to chaos.

A bifurcation diagram obtained from global continuation of six different limit cycles for $\tau = 0.59(s)$ is sketched in Fig. 1. The figure shows the transition from each of these cycles to chaos via a two-torus phase. It is important to note that chaotic and non-chaotic attractors coexist for the same parameters values.

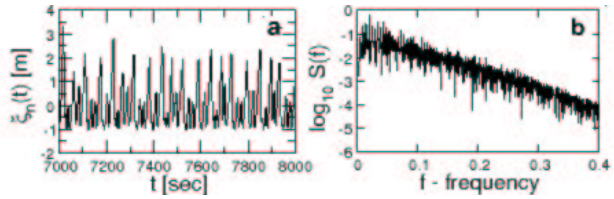

Fig. 2. **a** – $\xi_n(t)$ for $n = 10$, $\kappa = 15$, $\tau = 0.59(s)$ and $\rho = 0.1387(m^{-1})$. **b** – the corresponding power spectrum.

Fig. 2**a** shows the $\xi_n(t)$ time series for $\kappa = 15$, $\rho = 0.1387(m^{-1})$ and an arbitrarily chosen n. Fig. 2**b** presents the corresponding power spectrum. Its exponential decay is a sign of chaotic behavior of our system [10].

Another indication of chaos is the existence of positive Lyapunov exponents. A direct calculation of the largest Lyapunov exponent [11] and the Lyapunov exponents spectrum [12] yields three positive Lyapunov exponents of order 10^{-4}.

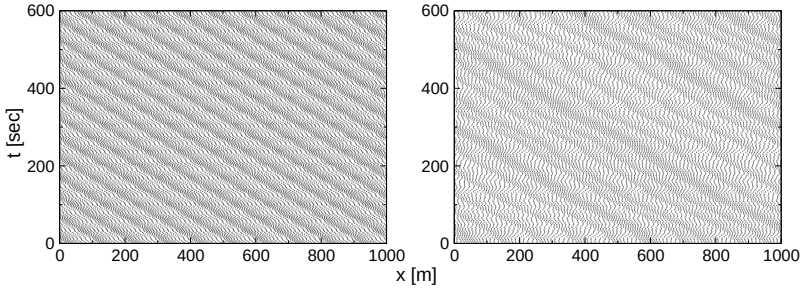

Fig. 3. Space-time diagrams of the traffic flow for $\kappa = 10$ and $\rho = 0.1(m^{-1})$. Left - $\tau = 0.4(s)$ (a limit cycle); right - $\tau = 0.59(s)$ (chaos). Each dot corresponds to a car.

As observed in real traffic, jams usually move in upstream direction. Our model reproduces this phenomenon. Fig. 3 presents space-time diagrams for the traffic flow for the cases of the system is on a limit cycle and on a chaotic attractor. One can clearly observe jams moving upstream, but in the chaotic

case they are not regular and perhaps look more similar to what can be observed on the road.

3 Multifractality Analysis

The chaoticity of an attractor can also be characterized by its fractal dimensions. We consider the correlation function of the moment q

$$C_q(r) = \left[\frac{1}{M} \sum_{i=1}^{M} \left[\frac{1}{M} \sum_{j=1}^{M} \Theta\big(r - |\mathbf{x}_i - \mathbf{x}_j|\big) \right]^{q-1} \right]^{\frac{1}{q-1}}, \tag{6}$$

where $\mathbf{x}_i = (\xi_n(t_i), \xi_n(t_i + \Delta t), \ldots, \xi_n(t_i + (d-1)\Delta t))$ are d-dimensional vectors (d is called embedding dimension), Δt is the the first zero of the time series autocorrelation function, Θ is the Heaviside step function and M is the time series length, which should be sufficiently large. The correlation dimension D_q is defined by the relation $C_q(r) \sim r^{D_q}$ (see [13,14] and references therein for more details).

To find the correlation dimensions numerically we use the algorithm proposed in [14]. Using these dimensions one can obtain the $f(\alpha)$ function [15], which represents the spectrum of fractal dimensions of the attractor.

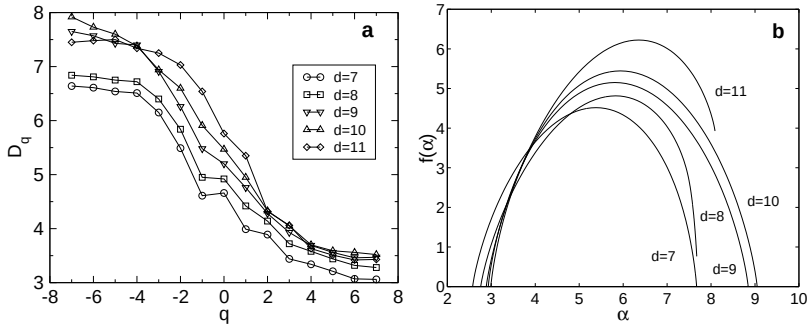

Fig. 4. a. Results of measurement of the correlation dimension D_q for $q = -7..7$ and $d = 7..11$ (bottom to top). **b**. Approximate $f(\alpha)$ fits for these data.

Fig. 4**a** shows the results of measurements of D_q for $q = -7..7$ and $d = 7..11$. Fitting these data with a continuous function $D(q)$ for each d, we find the $f(\alpha)$ function according to the formula

$$f(\alpha(q)) = q\alpha(q) - \tau(q),$$

where $\tau(q) = (q-1)D(q)$ and $\alpha(q) = d\tau/dq$ (see e.g. [15]).

As can be observed from Fig. 4**a**, the values of D_q show weak convergence with growing q, especially for d close to 0. Therefore, presented values of dimensions may be underestimated. Nevertheless, shapes of $f(\alpha)$ for each d enable us to claim the multifractality of the considered attractor.

References

1. B.S. Kerner, H. Rehborn: Phys. Rev. E **53**, R4275 (1996) B.S. Kerner, H. Rehborn: Phys. Rev. Lett. **79**, 4030 (1997) B.S. Kerner: Physics World 12 (August), 25 (1999)
2. P.S. Addison, D.J. Low: Chaos **8**, 791 (1998) D.J. Low, P.S. Addison: Nonlinear Dynamics **16**, 127 (1998)
3. T. Nagatani: Phys. Rev. E **60**, 1535 (1999)
4. M. Bando, K. Hasebe, A. Nakayama, A. Shibata, Y. Sugiyama, Phys. Rev. E **51**, 1035 (1995) Y. Sugiyama. In: *Proceedings of Workshop on Traffic and Granular Flow (1995, Julich)*, ed. by D.E. Wolf, M. Schreckenberg, A. Bachem (World Scientific, Singapore 1996)
5. E. Tomer, L. Safonov, S.Havlin: Phys. Rev. Lett. **84**, 382 (2000)
6. E. Tomer, L. Safonov, and S. Havlin. In: *Traffic and Granular Flow '99: Socilal, Traffic and Granular Dynamics*, ed. by D. Helbing, H.J. Herrmann, M. Schreckenberg, D.E. Wolf (Springer, Heidelberg/Berlin 2000), p. 419-424
7. L.A. Safonov, E. Tomer, V.V. Strygin, S. Havlin: Physica A **285**, 147 (2000)
8. L.A. Safonov, E. Tomer, V.V. Strygin, Y. Ashkenazy, S. Havlin: Europhys. Lett., in press (2001)
9. S. Newhouse, D. Ruelle, F. Takens: Commun. Math. Phys. **64**, 35 (1978) D. Ruelle, F. Takens, Commun. Math. Phys. **20**, 167 (1971)
10. H.G. Schuster, *Deterministic Chaos: An Introduction* (VCH, Weinheim 1995)
11. M.T. Rosenstein, J.J. Collins, C.J. De Luca: Physica D **65**, 117 (1993)
12. A. Wolf, J.B. Swift, H.L. Swinney, A. Vastano: Physica D **16**, 285 (1985)
13. P. Grassberger, I. Procaccia: Physica D **9**, 189 (1983) K. Pawelzik, H.G. Schuster: Phys. Rev. A **35**, 481 (1987)
14. Y. Ashkenazy: Physica A **271**, 427 (1999)
15. C.J.G. Evertsz, B.B. Mandelbrot, 'Multifractal measures.' In: H.-O. Peitgen, H. Jürgens, D. Saupe *Chaos and Fractals. New Frontiers of Science* (Springer-Verlag, New York 1992), pp. 921-944